KSTLE International Journal, Vol. 1, No. 2, December 2000, pp. 83-90

Surface Roughness Effects on the Lubrication Characteristics of the Engine Piston Ring Pack

Jeong-Eui Yun†

Department of Automotive Engineering, Donghae University 199 Jiheung-dong, Donghae, Kangwondo 240-713, Korea

Abstract : The surface roughness between a piston ring pack and a cylinder liner directly affects the fuel economy, the oil consumption, and the emission of the engine so that it is very important to clarify the surface roughness effects on the lubrication characteristics. The friction characteristics of the piston ring during engine operations are known to as mixed lubrication experimentally. In this study to simulate the effects of the surface roughness of the piston ring pack on the lubrication characteristics, the mixed lubrication analysis of piston rings was performed using the simplified average Reynolds equation. From the results the surface roughness was found be considerably affects minimum oil film thickness as well as FMEP(Friction Mean Effective Pressure). Especially, the oil ring was the most sensitive on the surface roughness.

Key words : piston ring, friction, oil film thickness, mixed lubrication

Introduction

Approximately 30 to 70% of the mechanical losses in a reciprocating engine are contributed by the friction at the piston ring and the cylinder interface [1-4]. The friction characteristics of a piston ring are influenced by the structure of an engine, the shape of a piston and piston ring and engine operating conditions etc. Therefore, the lubrication analysis of a piston ring assembly through the numerical simulation can be useful tool for an optimized design of a piston ring assembly because all of its characteristic behavior cannot be investigated experimentally.

Since Cattleman [5] first calculated the oil film thickness using the hydrodynamic lubrication theory, many theoretical analysis for a piston ring have been carried out using the Reynolds equation [6,7], which is a traditional equation for hydrodynamic lubrication. Numerous automotive researchers have revealed that the piston ring clearly shows mixed lubrication characteristics near TDC and BDC of each stroke from the experimental studies using commercial engines [8-11]. Rhode [12] attempted to analyze the lubrication characteristics of a piston ring assembly through the use of mixed lubrication model. His model was based on average Reynolds equation, which was reconstructed from Reynolds equation by Patir and Cheng [13,14] considering the effect of surface roughness. It has been applied over the decade for an analysis of the piston ring assembly to obtain desirable results [15,16]. However, average Reynolds equation requires an additional calculation of average gap ($\bar{h}_T$), which considers the asperity contact between two lubricated surfaces.

In this study the mixed lubrication analysis of the piston ring was performed using simplified average Reynolds equation, which was originally presented by Wu and Zheng [17] introducing a contact factor for the reduction of the complicate numerical calculation. The numerical procedure and calculation time required for modeling and analysis was significantly reduced since this equation was expressed only in terms of nominal film thickness (h). After this model was confirmed comparing simulation results to measured results, we applied this model to piston ring pack lubrication analysis to clarify the effects of surface roughness.

†Corresponding author; Tel: 82-33-521-9900; Fax: 82-33-521-9407
E-mail: jeyun@mail.tonghae.ac.kr

Mixed Lubrication Model of Piston Ring

Patir and Cheng [13,14] presented the average flow model, which was reconstructed from traditional Reynolds equation by introducing flow factors (ϕ_x, ϕ_y, ϕ_z) in order to consider the effect of lubricated surface roughness. Their average Reynolds equation is as follows.

$$\frac{\partial}{\partial x}\left(\phi_x \frac{h^3}{12\mu}\frac{\partial p}{\partial x}\right)+\frac{\partial}{\partial y}\left(\phi_x \frac{h^3}{12\mu}\frac{\partial p}{\partial y}\right) \tag{1}$$

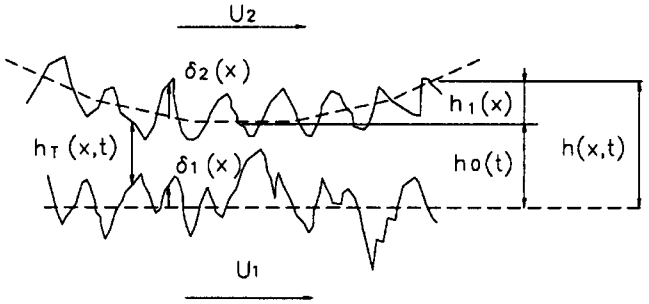

Fig. 1. Film thickness function.

$$= \frac{U_1 + U_2}{2}\frac{\partial \bar{h}_T}{\partial x} + \frac{U_1 - U_2}{2}\sigma\frac{\partial \phi_s}{\partial x} + \frac{\partial \bar{h}_T}{\partial t}$$

In order to evaluate oil film pressure from above equation, the calculation of the average gap ($\bar{h}_T$) shown in Fig. 1 is required as well as nominal film thickness (h). The average gap that considers the asperity contact between lubricated surfaces is defined as follow.

$$\bar{h}_T = \int_{-h}^{\infty}(h+\delta)f(\delta)d\delta \tag{2}$$

Wu and Zheng [17] introduced the contact factor defined below to eliminate this additional effort.

$$\phi_c = \frac{\partial \bar{h}_T}{\partial h} = \int_{-H}^{\infty}\varphi(s)ds \tag{3}$$

Therefore Equation (1) can be written as follows.

$$\frac{\partial}{\partial x}\left(\phi_x\frac{h^3}{12\mu}\frac{\partial p}{\partial x}\right) + \frac{\partial}{\partial y}\left(\phi_y\frac{h^3}{12\mu}\frac{\partial p}{\partial y}\right) = \phi_c\left(\frac{U_1 + U_2}{2}\frac{\partial h}{\partial x} + \frac{\partial h}{\partial t}\right) + \frac{U_1 - U_2}{2}\sigma\frac{\partial \phi_s}{\partial x} \tag{4}$$

For the application of Equation (4) into the lubrication analysis of the piston ring assembly, oil film thickness between the piston ring and the cylinder wall is assumed as an infinite flat bearing. And it is also assumed that the piston ring is fixed and the cylinder wall moves with a velocity of U. Then Equation (4) can be reduced like following form.

$$\frac{d}{dx}\left(\phi_x\frac{h^3}{12\mu}\frac{dp}{dx}\right) = \phi_c\left(\frac{U}{2}\frac{dh}{dx} + \frac{dh}{dt}\right) + \frac{U}{2}\sigma\frac{d\phi_s}{dx} \tag{5}$$

with $p(0,t) = p_T(t)$, $p(L,t) = p_B(t)$

Oil film thickness can be expressed in terms of a ring face profile and a time variant term as shown in Fig. 1.

$$h(x,t) = h_o(t) + h_l(x) \tag{6}$$

Numerical Analysis

Geometry of lubricated conjunction between the piston ring and the cylinder bore is shown in Fig. 2. The oil viscosity within the ring width is assumed as a constant and dimensionless variables shown below are introduced to simplify the calculation.

$$\bar{x} = x/L \quad H = h/\sigma$$
$$\bar{t} = t\omega \quad \bar{h}_0 = h_0/\sigma$$
$$\bar{p} = p/p_0 \quad \bar{h}_1 = h_1/\sigma \tag{7}$$
$$\bar{\mu} = \mu/\mu_0 \quad \bar{U} = U/U_0$$

Equation (5) can be rearranged in terms of these variables as follows.

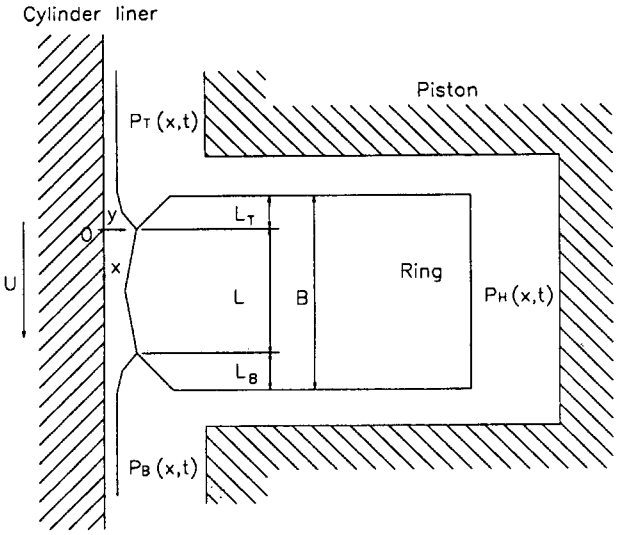

Fig. 2. Geometry of lubricated conjunction between piston ring and cylinder wall.

$$\frac{d}{d\bar{x}}\left(\phi_x H^3\frac{d\bar{p}}{d\bar{x}}\right) = \bar{\mu}\bar{U}\left(\phi_c\frac{dH}{d\bar{x}} + \frac{d\phi_s}{d\bar{x}}\right) + 2\frac{L}{R_c}\bar{\mu}\phi_c\frac{dH}{d\bar{t}} \tag{8}$$

with $\bar{p}(0,\bar{t}) = \bar{p_T}(\bar{t}), \bar{p}(1,\bar{t}) = \bar{p_B}(\bar{t})$

Double integration with respect to x using above boundary conditions gives following result.

$$\bar{p}(\bar{x},\bar{t}) = \bar{p_T}(\bar{t}) + (\bar{p_B}(\bar{t}) - \bar{p_T}(\bar{t}))\frac{I_3(\bar{x},\bar{t})}{I_3(1,\bar{t})} + \bar{\mu}\bar{U}\left(I_2(\bar{x},\bar{t}) - I_2(1,\bar{t})\frac{I_3(\bar{x},\bar{t})}{I_3(1,\bar{t})}\right) + 2\frac{L}{R_c}\bar{\mu}\frac{dH}{d\bar{t}}\left(I_1(\bar{x},\bar{t}) - I_1(1,\bar{t})\frac{I_3(\bar{x},\bar{t})}{I_3(1,\bar{t})}\right) \tag{9}$$

where

$$I_1(\bar{x},\bar{t}) = \int_0^{\bar{x}}\frac{\phi_c\xi}{\phi_x H^3}d\xi$$
$$I_2(\bar{x},\bar{t}) = \int_0^{\bar{x}}\frac{1}{\phi_x H^3}\left(\int_0^H \phi_c dH + \phi_s\right)d\xi \tag{10}$$
$$I_3(\bar{x},\bar{t}) = \int_0^{\bar{x}}\frac{1}{\phi_x H^3}d\xi$$

However, the oil film pressure ($\bar{p}$) in Equation (9) cannot be found unless additional information on oil film thickness (H, $dH/d\bar{t}$) are provided. Therefore a following force equilibrium condition is used on the radial direction of a ring to find a possible constraint.

$$F_T = F_{c,oil} + F_{c,asp} + F_{g,pre} + F_{r,ten} = 0 \tag{11}$$

The oil resistance force ($F_{c,oil}$) in Equation (11) which occurs from the oil film can be obtained by applying Half Sommerfeld boundary condition.

$$F_{c,asp} = 2\pi RLp_0\int_0^1 \bar{p}\chi(\bar{p})d\bar{x} \tag{12}$$

$$\chi(\bar{p}) = 0 \quad for \quad \bar{p} < 0$$

$$1 for \quad \bar{p} \geq 1$$

The contact asperity force ($F_{c,asp}$) in Equation (11) between a ring and a cylinder wall was obtained from an integration using Greenwood and Tripps equation [18] shown in Equation (14) and (15). They derived the contact force per unit area (P_{AC}) and contact area (A_{AC}) within the range of elastic deformation, which occurs at the asperity contact on plate with two rough surfaces of Gaussian distribution.

$$F_{c,asp} = 2\pi RLp_0\int_0^1 \bar{p}\chi(\bar{p})d\bar{x} \tag{13}$$

$$P_{AC}(h) = \frac{\sqrt[6]{2}}{15}\pi(\eta\beta\sigma)^2 E\sqrt{\frac{\sigma}{\beta}}F_{5/2}\left(\frac{h}{\sigma}\right) \tag{14}$$

$$A_{AC}(h) = \pi^2(\eta\beta\sigma)^2 F_2\left(\frac{h}{\sigma}\right) \tag{15}$$

$$\text{where } F_n\left(\frac{h}{\sigma}\right) = \frac{1}{\sqrt{2\pi}}\int_{h/\sigma}^{\infty}\left(S-\frac{h}{\sigma}\right)^n e^{-\frac{S^2}{2}}dS \tag{16}$$

Nonlinear functions given in Appendix are used to reduce the computation time in this numerical modeling.

The force caused by the boundary pressure ($F_{l,pre}$) at the region exposed to the gas is defined as follows.

$$F_{l,pre} = 2\pi R(p_T L_T + p_B L_B) \tag{17}$$

The force due to the gas pressure ($F_{g,pre}$) behind the ring can be written as follows.

$$F_{g,pre} = 2\pi p_H(R\text{-}R_{GWD})B \tag{18}$$

Similarly, the force caused by the ring tension ($F_{r,ten}$) can be expressed as follows.

$$F_{r,ten} = Krh \tag{19}$$

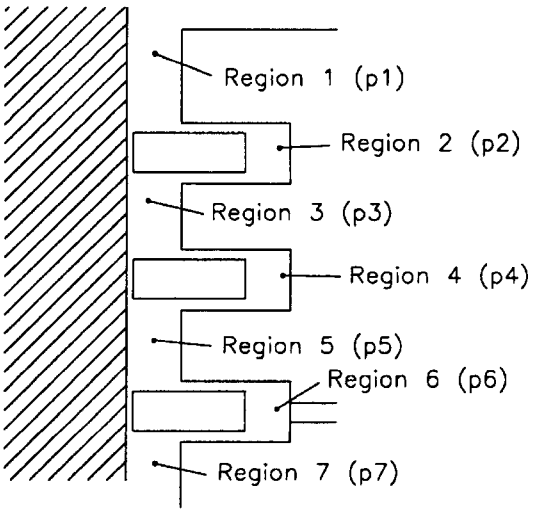

Fig. 3. Schematic of piston-cylinder-ring crevice region and gas pressure.

Oil film pressure and thickness can be computed applying iteration method into Equation (9) and (11). That is, it is calculated from Equation (9) with the appropriate initial values of (h_0) and (dh_0/dy) and the convergence of (F_T) needs to be checked.

$$|F_T| < \varepsilon_1 \tag{20}$$

Iterations should be continued until the following condition is satisfied:

$$|h_0(t) - h_0(t+\tau)| < \varepsilon_2 \tag{21}$$

Ring friction is computed through the use of oil film thickness and pressure calculated from Equation (9) and (11). Generally, it occurs by the combination of two different friction mechanism: One is viscous friction (F_v) caused by the shear force of oil between ring and cylinder wall, and another is boundary friction (F_b) brought by the asperity shear force between lubricated surfaces [15,16]. Viscous friction and boundary friction can be obtained from equations below (refer to Appendix).

$$F_v = 2\pi R\int_0^L \tau_h dx \tag{22}$$

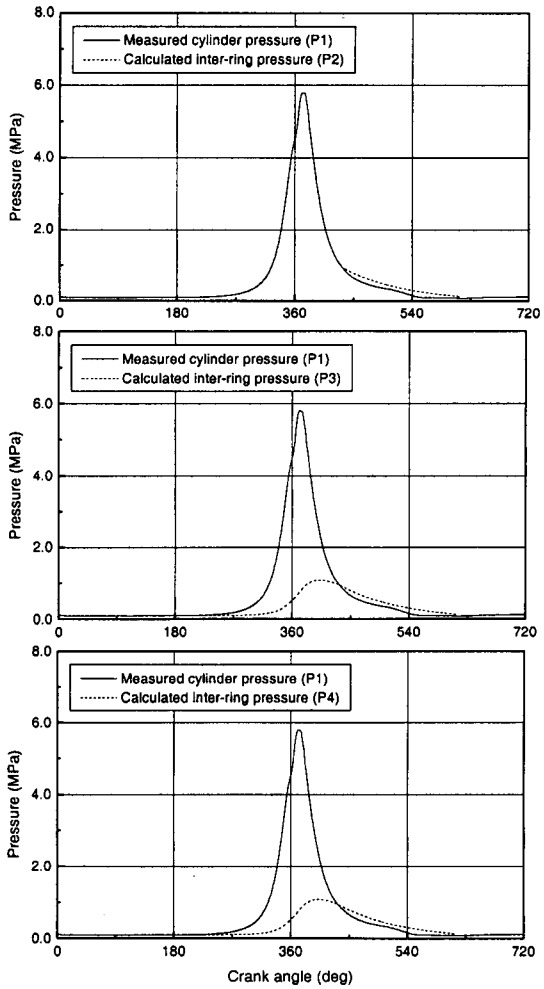

Fig. 4. Inter-ring gas pressure acting on rings (Full load 3000 rpm).

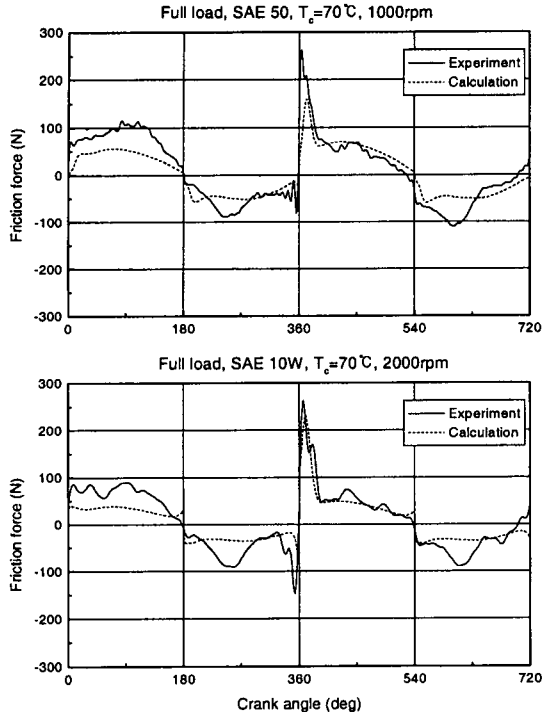

Fig. 5. Comparison between experimental and analytical results.

$$\tau_h = -\frac{\mu U}{h}(\phi_f + (1-2V_{r2})\phi_{fs}) + \frac{dp}{dx}\left(h\phi_{fp}\left(\frac{1}{2}+V_{r2}\right) - V_{r2}\bar{h}_t\right) \quad (23)$$

$$F_b = \tau_0 A_C + \alpha W_c \quad (24)$$

$$A_C = 2\pi R\int_0^L A_{AC}(h)dx \quad (25)$$

$$W_C = 2\pi R\int_0^L P_{AC}(h)dx \quad (26)$$

According to Equation (23), τ_h has to be infinity, as the oil film thickness becomes infinitely thin. Rhode [12] reported that the oil cannot endure and infinite shear force under the infinitesimally thin oil film thickness, and introduced an experimental equation shown in Equation (27) to get rid of the contradiction in Equation (23).

$$\tau_c = \tau_0 + \alpha p \quad (27)$$

In this study, ring friction was calculated assuming that $|\tau_h| = |\tau_c|$ is maintained even if $|\tau_h| > |\tau_c|$.
The specifications of the ring assembly used in this study are shown in Table A-1.

Inter-ring gas pressures (P_2, P_3, P_4) shown in Fig. 3 were computed from the observed cylinder pressure (P_1). Gas pressures below second ring (P_5, P_6, P_7) were assumed as the atmospheric pressure. Fig. 4 exhibits the variation of inter-ring gas pressure, which is used as boundary conditions (p_T,p_B) in the lubrication analysis.

Results and Discussions

Fig. 5 shows the comparison between experimental [11] and analytical friction forces. From this figure, we can see that analytical results very well predict boundary friction in the TDC region for 1000 and 2000 rpm respectively. However there is a little difference in the middle stroke. It seems to be originated from exclusion of piston skirt friction in the analytical results. The plotted experimental friction included the skirt friction force as well as the ring pack friction force [11], but the analytical results were obtained from only the ring pack friction force. It is well known that the skirt friction force has fully hydrodynamic friction characteristics, so that its friction force is maximized at the middle stroke and minimized at the TDC and BDC region due to the velocity effect.

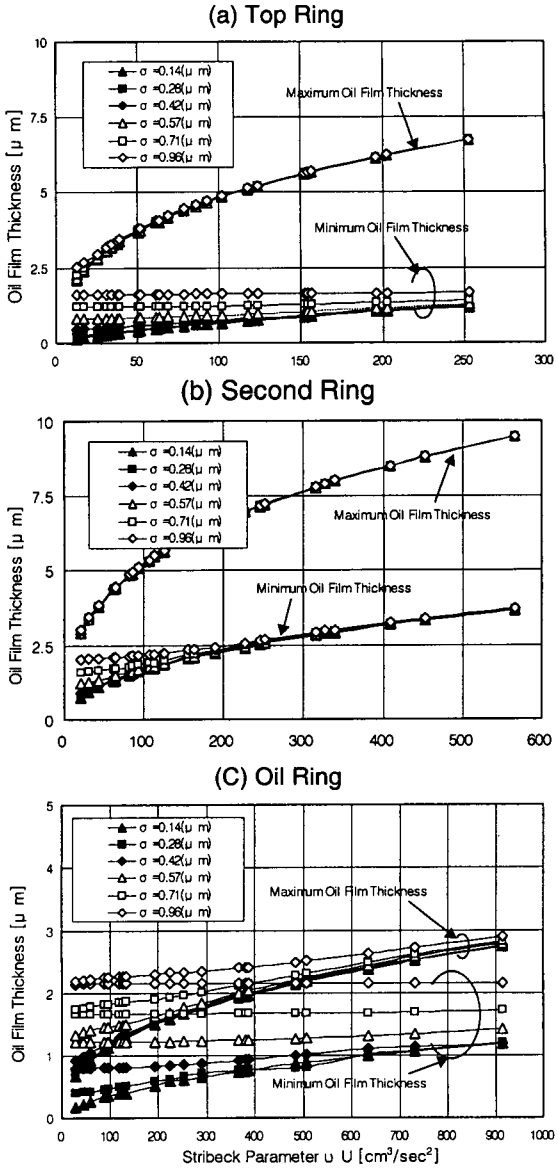

Fig. 6. Surface roughness effects on maximum and minimum oil film thickness against Stribeck parameter.

Fig. 6 shows surface roughness effects on the minimum and maximum oil film thickness during 1 cycle. In case of the second ring, maximum oil film thickness is not affected by the surface roughness in the simulation range, from 0.14 to

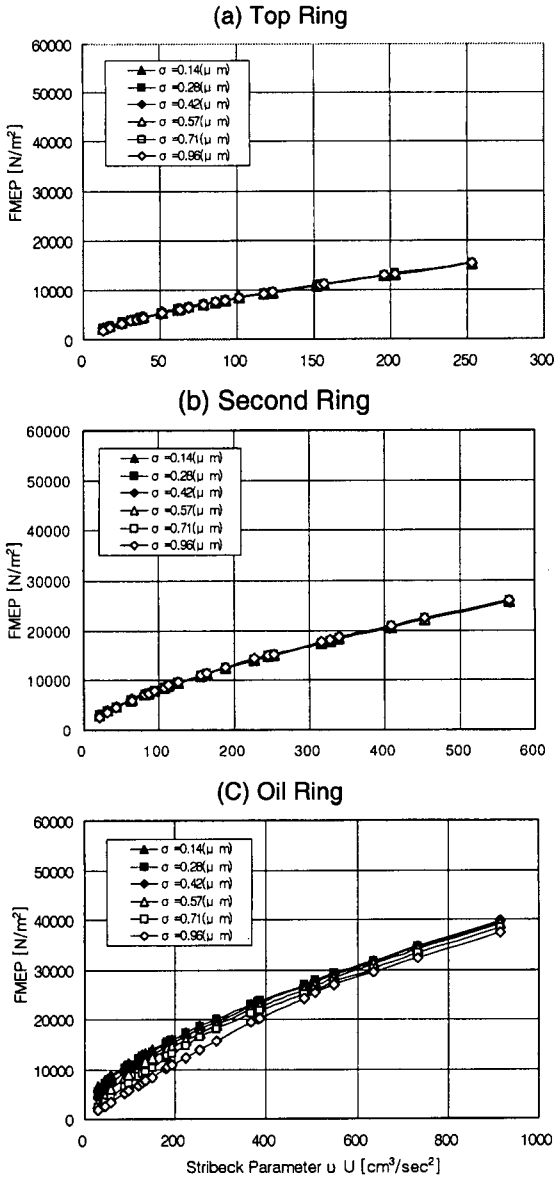

Fig. 7. Surface roughness effects on viscous friction friction component of total FMEP at each ring.

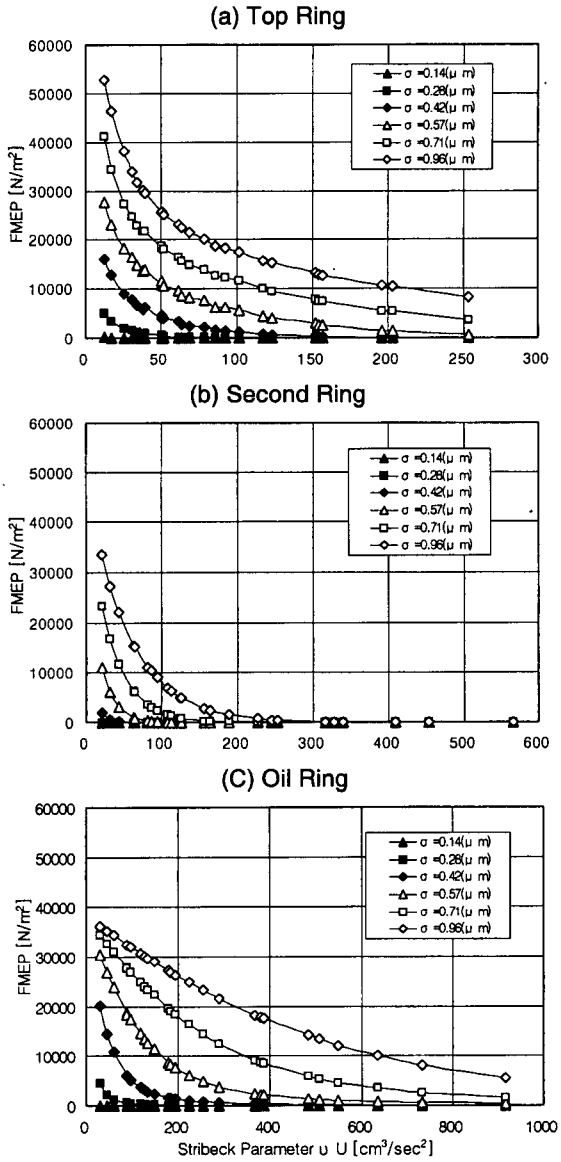

Fig. 8. Surface roughness effects on boundary friction force component of total FMEP at each ring.

0.96 μm. It just shows typical hydrodynamic lubrication behavior, in which it increases with increase of Stribeck parameter, υU. But minimum oil film thickness is influenced by the surface roughness below specific Stribeck parameter value, 300 υU(cm^3/sec^2). However this effect also disappears with increase of Stribeck parameter. In case of the top ring, the surface roughness affects the maximum as well as minimum oil film thickness, that is to say, oil film thickness of the top ring is more sensitive than the second ring. The reason seems to be inter-ring pressure. The main load on the lubricating surface is gas pressure, and the gas pressure acting behind the top ring is more than that of the second ring as described in Fig. 4. On the other hand, in case the oil ring, the trend of oil film thickness variation with surface roughness is considerably different from the others. The order of the oil film thickness is the smallest, so that the surface roughness between the ring and liner interface seriously affects the oil film thickness in the whole range of the simulation. The reason why the oil ring is influenced by surface roughness is because the width of the oil ring is the smallest, so that oil film thickness is not built enough to overcome asperity contact.

Fig. 7 shows the viscous friction component of the total FMEP at each ring, In case of the top and the second ring, the viscous component of the total FEMP is not affected by the surface roughness because the oil film thickness is larger than 3 times of surface roughness. But the hydrodynamic component of the total FEMP in the oil ring is slightly affected by the surface roughness. In that case, the hydrodynamic component of the total FEMP decreases with increase of surface roughness. These results may be estimated by the results of previous information for oil film thickness. In that case maximum and minimum oil film thickness increases with increase of surface roughness. As a result, increased oil film

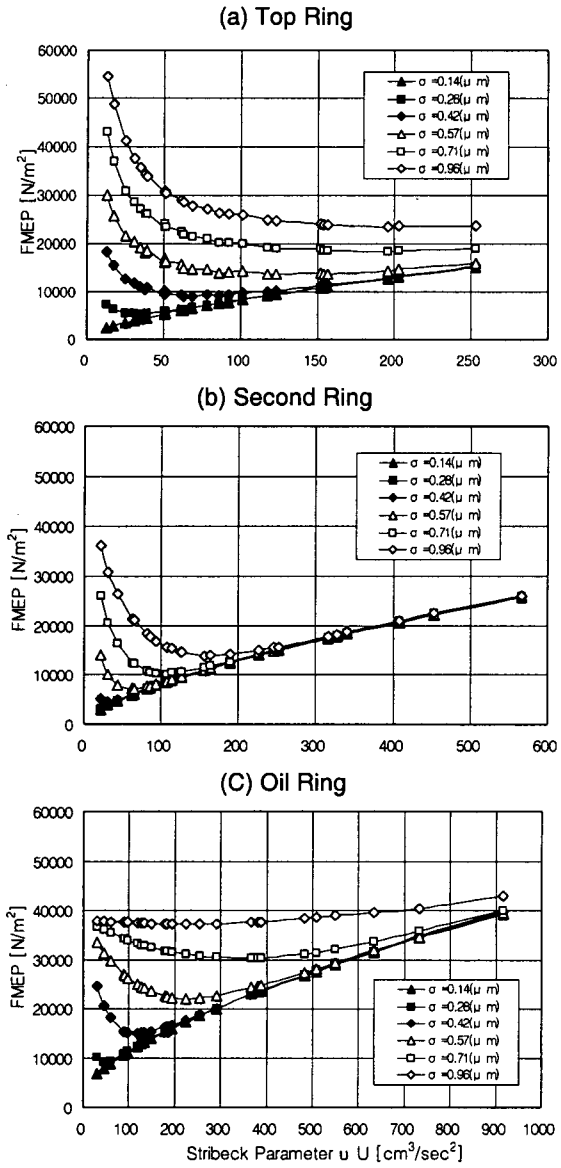

Fig. 9. Surface roughness effects on total friction force component of total FMEP at each ring.

thickness results in decrease of viscous friction component.

Fig. 8 indicates the boundary friction components of the total friction force due to the asperity contact. In all cases the friction shows the typical trend in which it sharply decreases with increase of Stribeck parameter. Especially, we can see that the boundary friction component of the top ring is larger than that of he second ring. This result comes from the gas pressure behind ring as mentioned at the previous figure. Generally, the higher-pressure acting behind the ring pushes the ring to the cylinder wall more closely. Therefore the asperity contact between the ring and cylinder wall is generated more frequently.

Fig. 9 shows the total FMEP of each ring. As shown in these figures, in case of surface roughness is 0.14 μm, the total FMEP of all the ring shows the hydrodynamic behavior in which FMEP increases with increase of vU. While in case of surface roughness is more than 0.14 μm, the total FMEP shows the typical mixed lubrication characteristics.

Conclusions

In this study to simulate the effects of the surface roughness of the piston ring pack on the lubrication characteristics, the mixed lubrication analysis of piston rings was performed using the simplified average Reynolds equation. Through the simulated results the surface roughness was found be considerably affects minimum oil film thickness as well as friction force. Especially, the oil ring was the most sensitive on the surface roughness.

Nomenclature

A_{AC}	real contact area of asperity per unit area [-]
A_C	real contact area of surface asperity [m²]
B	ring thickness [m]
E	elasticity of two lubricated surfaces [N/m²]
K_r	spring constant [N/m]
h	nominal film thickness [m]
h_0	time dependent minimum oil film thickness [m]
h_1	lubricated surface profile of ring [m]
$\overline{h_T}$	average gap [m]
h_T	local film thickness [m]
L	lubricated surface of ring [m]
L_T, L_B	ring surface exposed to gas of top and bottom [m]
p	oil film pressure [N/m²]
p_T, p_B	gas pressure at top and bottom [N/m²]
p_H	gas pressure behind ring [N/m²]
p_{AC}	asperity contact force of lubricated surface per unit area [N/m²]
R	bore radius [m]
R_C	crank radius [m]
R_{GWD}	ring width [m]
U	velocity of lubricated surface [m/sec]
U_0	piston speed(= ωR_C)
W_C	asperity contact force of lubricated surface [N/m²]
ε_1	radius of convergence for $\frac{dh_0}{dt}$
ε_2	radius of convergence for $h_0(t)$
β	mean curvature of radius at asperity vertex of lubricated surface [m]
$\lambda_{0.5}$	0.5 correlation length of profile
γ	surface pattern parameter ($\gamma = \lambda_{0.5x}/\lambda_{0.5y}$) [-]
δ_1,δ_2	roughness amplitudes of surfaces 1 and 2 [m]
δ	combined roughness ($\delta_1 + \delta_2$) [m]
$f(\delta)$	probability density function of combined roughness
η	asperity density of lubricated surface [1/m²]
μ	oil viscosity [N/(m²sec)]
μ_0	referenced viscosity [N/(m²sec)]
σ_1,σ_2	RMS roughness of lubricated surface [m]
σ	average RMS roughness of two lubricated surfaces (= $\sigma^2_1 + \sigma^2_2$)
V_{r1},V_{r2}	variance ratio of surface roughness [-]
τ_c	contact shear stress of surface asperity [N/m²]

τ_h shear stress of lubricant [N/m^2]
τ one cycle of engine [=720^0]
ϕ_x, ϕ_y, ϕ_z pressure flow factors [-]
ϕ_c contact factor [-]
$\phi_f, \phi_{fs}, \phi_{fp}$ shear stress factors [-]
ω angular velocity of engine [rad/sec]
$\varphi(s)$ standard probability density function of surface asperity [-]

References

1. McGeehan. J. A., A Literature Review of the Effects of Piston and Ring Friction an Lubricating Oil Viscosity on Fuel Economy, SAE Trans., Vol. 87. pp. 2619-2638, 1978.
2. Ting. L. L., A Review of Present Information on Piston Ring Tribology, SAE Trans., Vol. 17. pp. 1135-1146, 1985.
3. Hoshi. M., Reducing Friction Losses in Automobile Engines, Tribology International, Vol. 17. No. 4. pp. 185-189, 1984.
4. Hoshi. M. and Baba, Y., A Study of piston Friction Force in an Internal Combustion Engine. ASLE. Vol. 30, pp. 444-451, 1987.
5. Cattleman, R. A., A Hydrodynamic Theory of Piston Ring Lubrication, Physics. Vol. 7. pp. 364-367, 1936.
6. Ting, L. L. and Mayor, J. E., Piston Ring Lubrication and Cylinder Bore Wear Analysis. Part I-Theory. Journal of Lubrication Technology. pp. 305-314, 1974.
7. Rhode. S. M., Whitaker. K. W., and McAllister. G. T., A Study of the Effects of Piston Ring and Engine Design Variables on Piston Ring Friction. Energy Conservation Through Fluid Film Lubrication Technology: Frontiers in Research and Design. ASME. pp. 117-134, 1979.
8. Furuhama. S. and Sasaki. S., New Device for the Measurement of Piston Frictional Forces in Small Engines, SAE Trans., Vol. 92. pp. 781-792, 1983.
9. Takiguchi, M., Machida. K. and Furuhama. S., Piston Friction Force of a Small High Speed Gasoline Engine. ASME Trans., Vol. 110. pp. 112-118, 1988.
10. Wakuri, Y., Socjima, K., Kitahama. T., Nunotani. M. and Ootsubo, M., Studies on the characteristics of Piston Ring Friction, JSAE Review. Vol. 13. No. 2. pp. 48-53, 1992.
11. Yun, J. E. and Kim, S. S., New device for Piston Ring Assembly Friction Force Measurement in IDI Diesel Engine, JSME international Journal. Vol. 36. No. 4, 1983.
12. Rhode, S. M., A Mixed Friction Model for Dynamically Loaded Contacts with Application to Piston Ring Lubrication. Surface Roughness Effects in Hydrodynamic and Mixed Lubrication. ASME. pp. 19-50, 1980.
13. Patir. N. and Cheng. H. S., Application of Average Flow Model to Lubrication Between Rough Sliding Surfaces. Journal of Lubrication Technology, Vol. 101. pp. 220-230. 1979.
14. Patir. N and Cheng. H. S., An Average Flow Model for Determining Effects of three-dimensional Roughness on Partial Hydrodynamic Lubrication, Journal of Lubrication Technology, Vol. 100, pp. 12-17, 1978.
15. Richez. M. F. Costans. B. and Inquest. K., Theoretical and Experimental Study of Ring Liner Friction. Proc. 9th Leads-Lyon Symposium on Tribology. pp. 122-131, 1982.
16. Sanda. S. and Someya. T., The Effect of Surface Roughness on Lubrication Between a Piston Ring and a Cylinder Liner. Proc. IMechE., Vol. 1. pp. 135-143, 1987.
17. Wu. C. and Zheng. L., An Average Reynolds Equation for Partial Film Lubrication with a Contact Factor. Journal of Tribology. Vol. 111. pp. 188-191, 1989.
18. Greenwood. J. A. and Tripp. J. H., The Contact of Two Nominally Flat Rough Surfaces. Proc. IMechE., Vol. 185. pp. 625-633, 1971.

Appendix

Table 1. Specifications of a piston ring pack.

	Top Ring	2nd Ring	Oil Ring
Type	Barrel	Taped	2-Piece
Width	2.48mm	1.98mm	0.7mm
Thickness	3.7mm	3.8mm	2.4mm
Tension	19.61N	15.2N	32.85N

• Contact Factor

For Gaussian distribution:

$$\phi_c = e^{-0.6912 + 0.782H - 0.304H^2 + 0.04H^3} \quad for\ 0 \le H < 3$$

$$1 \quad for\ H \ge 3$$

For triangular distribution:

$$\phi_c = \frac{1}{2} + \frac{H}{\sqrt{6}} - \frac{H^2}{12} \quad for \quad 0 \le H < \sqrt{6}$$

$$= 1 \quad for \quad H > \sqrt{6}$$

• Flow Factor

$$\phi_c = \frac{35}{32} z((1-z^2)^3 \ln\frac{z+1}{\varepsilon^*} + \frac{1}{60}(-55+z(132+z(345+z(-160+z(-405+z(60+147z)))))) \quad for \quad z \le 1$$

$$\frac{35}{32} z(1-z^2)^3 \ln\frac{z+1}{z-1} + \frac{z}{15}(66+z^2(30z^2-8))) \quad for \quad z > 1$$

where $z = H/3$, $\varepsilon^* = \varepsilon/3\sigma$

$$\overline{h_T} = h \quad for \quad z \ge 1$$

$$\frac{3\sigma}{256}(35+z(128+z(140+z^2(28-5z^2)))) \quad for \quad z < 1$$

$$\phi_x = 1\text{-}ce^{-1rH} \quad for \quad \gamma \le 1$$
$$1+cH^r \quad for \quad \gamma > 1$$

$$\phi_s = V_{r1}\Phi_s(H,\gamma_1) - V_{r2}\Phi_s(H,\gamma^2)$$
$$\Phi_s = A_1 H^{\alpha_1} e^{-\alpha_2 H + \alpha_3 H^2} \quad for \quad H \le 5$$
$$A_2 e^{-0.25H} \quad for \quad H > 5$$

$$\phi_{fp} = 1\text{-}De^{-sH}$$

$$\phi_{fs} = V_{r1}\Phi_{fs}(H,\gamma_1) - V_{r2}\Phi_{fs}(H,\gamma_2)$$
$$\Phi_{fs} = A_3 H^{\alpha_4} e^{-\alpha_5 H + \alpha_6 H^2} \quad for \quad H \le 7$$
$$0 \quad for \quad H > 5$$

Table 2. Coefficients used in flow factor calculation.

	c	r	A_1	1	2	3	A_2	A_3	4	5	6	D	s
1/9	1.48	0.42	2.046	1.12	0.78	0.03	1.856	14.1	2.45	2.30	0.10	1.51	0.52
1/6	1.38	0.42	1.962	1.08	0.77	0.03	1.754	13.4	2.42	2.30	0.10	1.51	0.54
1/3	1.18	0.42	1.858	1.01	0.76	0.03	1.561	12.3	2.32	2.30	0.10	1.47	0.58
1	0.90	0.56	1.899	0.98	0.92	0.05	1.126	11.1	2.31	2.38	0.11	1.40	0.66
3	0.225	1.5	1.56	0.85	1.13	0.08	0.556	9.8	2.25	2.80	0.18	0.98	0.79
6	0.52	1.5	1.29	0.62	1.09	0.08	0.388	10.1	2.25	2.90	0.18	0.97	0.91
9	0.87	1.5	1.011	0.54	1.07	0.08	0.290	8.7	2.15	2.97	0.18	0.73	0.91

• Asperity Contact Function

$$F_n(H) = \begin{cases} c_1 e^{c_2 \ln(4-H)+c_3(\ln(4-H))^2} & \text{for } H \le 3.5 \\ c_4(4-H)^{c_5} & \text{for } 3.5 < H \le 4.0 \\ 0 & \text{for } H > 4.0 \end{cases}$$

Table 3. Constant values for $F_n(H)$.

	n=2	n=5/2
C_1	1.705E-4	2.1339E-4
C_2	4.05419	3.804467
C_3	1.37025	1.341516
C_4	8.8123E-5	1.1201E-4
C_5	2.1523	1.9447